

# Electrochemiluminescence detection of DNA Based on Signal Amplification Combined with Dendrimer Loaded Multiple Quantum Dots on Magnetic Nanoparticles

Xiaoxue Shi<sup>1,+</sup>, Feng Yang<sup>1,2,+</sup>, Changbing Pan<sup>3</sup>, Xiaoping Wei<sup>1,\*</sup>

<sup>1</sup> College of Chemical and Bioengineering, Guilin University of Technology, Guilin, Guangxi, 541004, China

<sup>2</sup> Haikou Marine Geological Survey Center, China Geological Survey, Haikou, China

<sup>3</sup> Affiliated Hospital of Guilin University of Technology, Guilin, Guangxi, 541004, China

\*E-mail: [xpwei@glut.edu.cn](mailto:xpwei@glut.edu.cn)

<sup>+</sup>these authors contributed equally to this work

Received: 2 December 2022 / Accepted: 15 January 2022 / Published: 6 June 2022

---

A new strategy was proposed for highly sensitive determined DNA determination by electrochemiluminescence method. Capture DNA of 5'-SH-ssDNA (DNA1) was immobilized on the Fe<sub>3</sub>O<sub>4</sub>@Au magnetic nanoparticles by self-assembly and attached on a magneto-controlled glass carbon electrode (MGCE). The capture DNA couple with the complementary end of the target DNA to form the dsDNA. The uncomplexed end of the target DNA continues hybrid with the probe DNA of 3'-NH<sub>2</sub>-ssDNA (DNA3) to form the sandwich-like dsDNA. Poly(DTPA-ethylene glycol)ester (PDTPA-EG) was synthesized and quantum dots were multiply loaded in the grid space of PDTPA-EG to form PDTPA-EG@CdTe nano-composites. The PDTPA-EG@CdTe nanoparticles were connected on the probe DNA by binding with the amino group of probe DNA. The ECL signal of quantum dots was recorded for quantitative analysis of target DNA. There was a linear relationship between the ECL intensity and the target DNA concentration in the range of  $1.0 \times 10^{-16} \sim 1.0 \times 10^{-14}$  mol/L, the detection limit was  $3.0 \times 10^{-17}$  mol/L. The sensitivity was dramatically enhanced with the help of multiple quantum dots loaded on PDTPA-EG.

---

**Keywords:** DNA, electrochemiluminescence, dendrimer, signal amplification, quantum dots

## 1. INTRODUCTION

The development of highly sensitive and selective methods for specific DNA sequence determination got more and more attentions for gene therapy and early diagnosis of diseases[1-3]. Compared with other detecting techniques such as fluorescence[4], surface plasma resonance spectra[5], quartz crystal microbalance[6] etc., electrochemiluminescence (ECL) method has the merits

of high sensitivity and selectivity, convenient, and strong capacities against interference[7,8]. There were many reports for the detect of DNA[9,10] by ECL methods and reagents commonly used are Ru(bpy)<sub>3</sub><sup>2+</sup> and luminol. But ruthenium compounds are very expensive, and luminol could only produce luminescence in the alkaline environment with H<sub>2</sub>O<sub>2</sub>. So the employment of these reagents is limited and the development of new ECL probes is necessary. Quantum dot(QD), which emission spectrum could be controlled according to its size dimension[11], has been widely reported as the ECL probe in DNA determination for its low oxidation potentials[12].

However, the intensity of the ECL signal is weak with one QD particle labeled, multiply labeled ECL probes has been employed for enhancing the intensity. Dendrimer is a material favored by researchers in recent years. It has excellent physical and chemical properties, good biocompatibility and chemical stability, etc., it has great potential applied in chemical and biological sensing[13]. Dendrimers can act as a carrier labeled with a large number of luminescent reagents to increase the ECL intensity of the detection[14]. The use of dendrimers to label luminescent reagents and QDs has been employed to develop highly sensitive immunoassay[15-17] and electrochemical sensors[18,19]. However, almost all dendrimers currently used for probe labeling are of the polyamide-amine(PAMAM)[20]. A large number of amino groups at the end of PAMAM might generate electrostatic binding with the electronegative DNA phosphate backbone[21], resulting in false positive signals. Furthermore, the use of the amino group at the end of the PAMAM cluster to bind the QDs also has problem of reduced the efficiency of electrochemiluminescence due to the different sizes of the QDs and the unstable binding of the QDs on the outer layer of PAMAM. We have synthesized a poly(diethylenetriaminepentaacetic acid-ethylene glycol) ester (PDTPA-EG) dendrimer with a three-dimensional network structure, and used it to multiply label luminol[22].

In this assay, the PDTPA-EG polymer with uniform spatial grid was used to synthesize CdTe QDs which doped in the grid of PDTPA-EG to get multi-probes labeling. The size of the QDs could be accurately controlled and stably immobilized, thereby improved the strength and stability of the ECL signal. As a result, an efficient ECL DNA determination method was established also with the help of the efficient separation and enrichment characteristics core-shell Fe<sub>3</sub>O<sub>4</sub>@Au. By the specific DNA hybridization, high sensitivity and high selectivity for the DNA determination results a good application prospects in the early diagnosis of cancer and gene sequence analysis.

## 2. EXPERIMENTAL

### 2.1 Apparatus and reagents

Cyclic voltammetry and electrochemiluminescence measurements were carried out on a Model MPI-E ECL analyzer systems (Xi'an Remex Instrument Co. Ltd, China) using a three-electrode system consisting of a platinum wire as the auxiliary electrode, an Ag/AgCl electrode as the reference electrode and a magnetic control Au electrode as working electrode. A Bransonic200 ultrasonic cleaning machine (Germany Branson Ultraschall Company), a pHS-2C model pH meter (Shanghai Leici Instruments, China), a RF-5301PC Fluorescence Spectrometer (Japanese Shimadzu Company)

and a TU-1901 double beam UV-visible light spectrophotometer (Beijing Purkinje General Instrument Co., Ltd) were also used. Other reagents were of analytical reagent grade. All solutions were prepared with doubly distilled water. DNAs of different sequences were purchased from Shenggong Bioengineering Company (Shanghai, China). The sequences of the oligoes were listed as follows:

Capture DNA(DNA1): 5'-SH-C<sub>6</sub>-AGT CAC TTA AAT-3'

Signal probe(DNA3): 5'-GGC CAG ATC GCG-C<sub>6</sub>-3'-NH<sub>2</sub>

Target DNA(DNA2): 5'-CGC GAT CTG GCC TGC ACA GTG ATT TAA GTG ACT-3'

Non complementary DNA (DNA4): 5'-TAT ACC TCT CGA TGC ACA GTG ATT TAA GTG ACT-3'

Three-base mismatch DNA(DNA5): 5'-TGT GTT CTG GCC TGC ACA GTG ATT TAA GTG ACT-3'

## 2.2 The synthesis of the core-shell Fe<sub>3</sub>O<sub>4</sub>@Au nanoparticles

According to the methods provided by references[23], the core-shell Fe<sub>3</sub>O<sub>4</sub> nanoparticles were prepared. FeCl<sub>3</sub>·6H<sub>2</sub>O and FeSO<sub>4</sub>·7H<sub>2</sub>O were dissolved in doubly distilled water with the molar ratio of Fe<sup>2+</sup>/Fe<sup>3+</sup> = 1:2 under N<sub>2</sub> atmosphere. Quick add 10 mL 25% ammonia water into the solution by fast agitation and then continue for 30 min. Rise the temperature to 80°C and maintained for 30 min. During the reaction process, the pH value was maintained at about 9. The black suspension was treated by ultrasound for 20 min, and then it was separated by magnet and washed by doubly distilled water till neutral. The residual was dissolved into 5mg/L solution and kept in volumetric flask.

0.229 g sodium citrate was dissolved in 100 mL water and heated. 1 mL above solution and 5 mL 10 mmol/L chloroauric acid were added into the solution by step when the temperature reached 99°C. Keep agitating with heat and without heat for 15 min separately. Finally the red brown solution was cooled under room temperature, separated by magnet and diluted to 20 mL. The Fe<sub>3</sub>O<sub>4</sub>@Au stock solution has to be preserved under 4°C for further use.

## 2.3 The Synthesis of the PDTPA-EG@CdTe

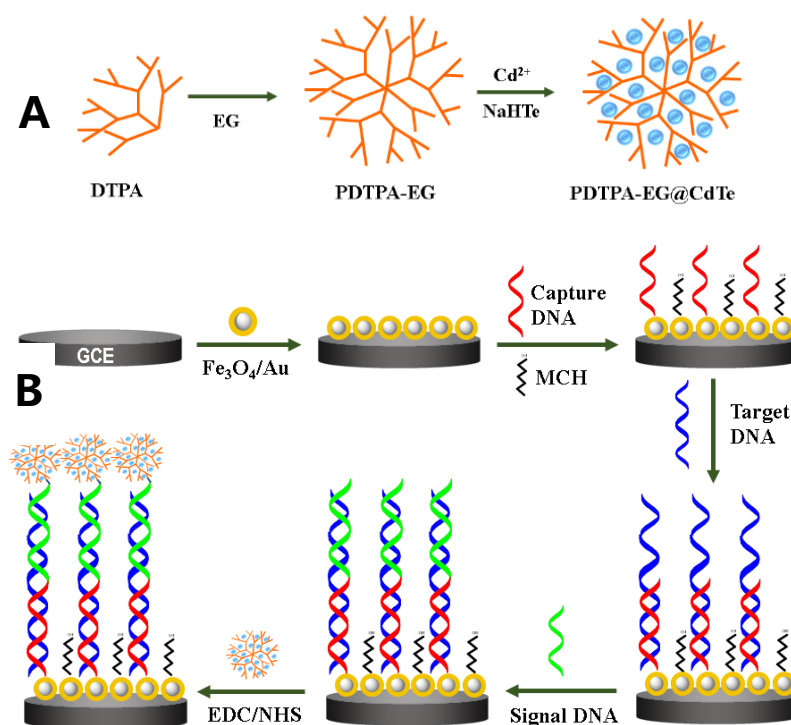
The PDTPA-EG dendrimer was synthesized according to the reference[24]. 50 mL four mouth flask equipped with a thermometer, a stirrer, a water knockout vessel and a spherical condenser pipe. 3.8 mmol DTPA (1.5 g), 20 mL dimethyl sulfoxide, 2 mL glycol and 3 mL pyridine were added in to the flask. 1mL stannous chloride (4.6 mg/mL, amount to excessive 10 times) was also added in. N<sub>2</sub> was purged all the time to expel air in the reaction system. Turned on the stirrer, rose temperature to 140~150°C for 5 h. After cooling to around 80°C, convert the system to reduced pressure distillation system. Adjusted the temperature to 100°C and the vacuum degree to 0.098 MPa and maintained the condition for 2 h to remove the solvent. Then the residual was cooled and a viscous brown-black PDTPA-EG dendrimer solution was obtained.

CdTe quantum dots were loaded on PDTPA-EG dendrimer to synthesize PDTPA-EG@CdTe nanocomposite according to the reference[16]. 0.024g Te powder, 0.032g NaBH<sub>4</sub> and 5 mL water were

added into a 50 mL three-neck flask. Stirred for 10 min at 60°C with N<sub>2</sub> as protecting gas and then got the NaHTe supernatant. 50 mL PDTPA-EG dendrimer solution was added into another 100 mL three-neck flask. Under N<sub>2</sub> atmosphere, CdCl<sub>2</sub> solution (M<sub>Cd<sup>2+</sup></sub>/M<sub>Te<sup>2-</sup></sub>=1:1) was added and vigorously stirred for 30 min. Then 800 μL NaHTe solution was added. The PDTPA-EG@CdTe nanocomposite could be obtained with heating circumfluence method at 100°C for 2 h. The synthesis steps were shown in Scheme 1A.

#### 2.4 Preparation of the modified electrodes

Firstly, 10 μL Fe<sub>3</sub>O<sub>4</sub>@Au was added onto the surface of the magnetically controlled glassy carbon electrode and then blew dry with N<sub>2</sub>. Then 10 μL 10 μmol/L sulfhydryl modified capture DNA and 40 μL 1 mol/L NaCl solution were added onto the electrode surface. The capture DNA could self-assemble onto the surface of the Fe<sub>3</sub>O<sub>4</sub>@Au nano particles by S-Au bond. In order to prevent the unspecific adsorption of the capture DNA, the electrode was immersed in 1 mmol/L 6-Mercapto-1-hexanol (MCH) and kept in dark for 2 h. Then the electrode was incubated in 0.5 mol/L NaCl solution containing target DNA. At last, a sandwich construction was formed by immersing the electrode 0.5 mol/L NaCl solution containing signal DNA for 1 h. The above electrode was then immersed in 2 mL 50 mg/mL EDC and NHS containing PDTPA-EG@CdTe solution for 1 h. All the incubation process was carried out on a shaking table rating 30 rpm. After that, the electrode was rinsed by PBS(pH7.4) and 1 mol/L NaCl solution for 3 times. This method was illustrated in Scheme 1B



**Scheme 1.** Scheme of synthesis of PDTPA-EG@CdTe (A) and ECL determination of DNA based on PDTPA-EG@CdTe label Fe<sub>3</sub>O<sub>4</sub>@Au nanoparticles (B)

### 2.5 Experimental method

The ECL test was conducted in 2 mL 0.1 mol/L PBS (pH 7.4) containing 0.1 mol/L  $K_2S_2O_8$  and 0.1 mol/L KCl at room temperature. The ECL measurement was performed from -2.0 to 0 V with the scan rate 100 mV/s. The voltage of photomultiplier tube (PMT) was set at 900 V.

## 3. RESULTS AND DISCUSSION

### 3.1 The UV-Vis adsorption spectrum of the PDTPA-EG and fluorescence spectrum of the PDTPA-EG@CdTe

The UV-Vis adsorption spectrum (curve a), Fluorescence adsorption spectrum (curve b) and Fluorescence emission spectrum (curve c) of the PDTPA-EG were shown in Fig. 1. As it can be seen, the maximum adsorption wavelength of the PDTPA-EG was about 220 nm, which is similar to that in the reference [25]. When the PDTPA-EG@CdTe was activated by the 360 nm light, its maximum emission wavelength was around 441 nm. It is also the same as that of reporting[26].

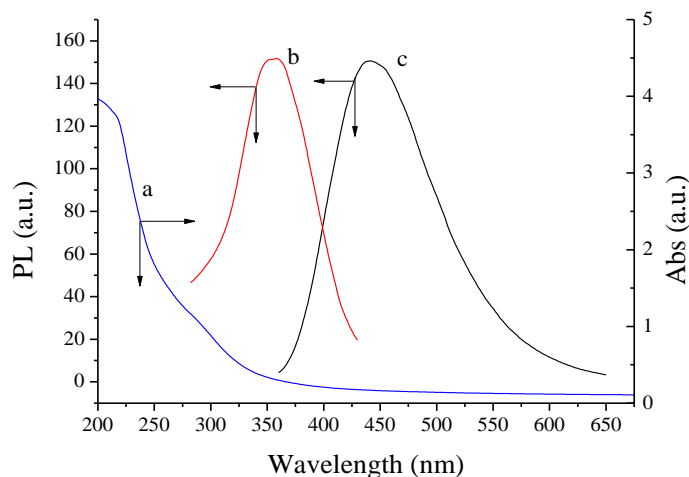


**Figure 1.** UV/vis absorption of PDTPA-EG (a), fluorescent excitation (b) and emission (c) spectra of PDTPA-EG@CdTe

### 3.2 The IR spectrum of the PDTPA-EG

The FT-IR spectrum was recorded by the FT-IR824 infrared spectrometer. The IR spectra of DTPA (curve a) and PDTPA-EG (curve b) were shown in Fig. 2.

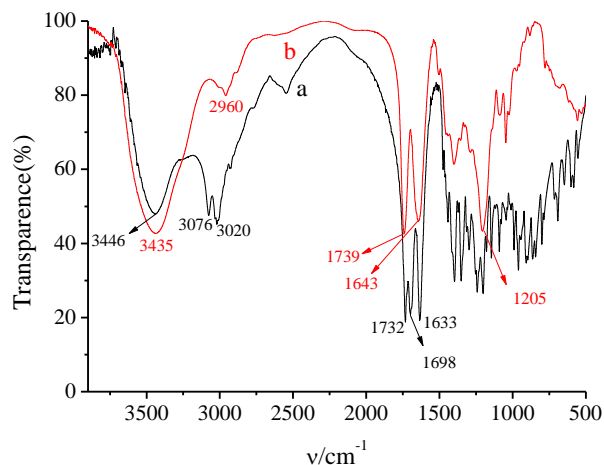


**Figure 2.** The infrared-spectrum of DTPA (a) and the complexes of PDTPA-EG (b)

The characteristic peaks of DTPA were  $3076\text{ cm}^{-1}$ ,  $3020\text{ cm}^{-1}$  (-OH stretching vibration),  $1732\text{ cm}^{-1}$ ,  $1698\text{ cm}^{-1}$  (C=O stretching vibration), after DTPA esterification (curve b), its characteristic peaks were mainly  $3435\text{ cm}^{-1}$ ,  $1739\text{ cm}^{-1}$  (C=O stretching vibration),  $1205\text{ cm}^{-1}$  (C-O-C stretching vibration). These characteristic peaks prove the existence of the ester structure as mentioned in references[18, 22].

### 3.3 The TEM characterization of PDTPA-EG@CdTe

As shown in Fig. 3, PDTPA had a grid structure with obvious characteristics, and the CdTe quantum dots were uniformly dispersed on the cavities and branches of the PDTPA dendrimers with a spatial grid structure. The size of CdTe quantum dots were uniform, with an average size of about 10 nm, and had good dispersion.

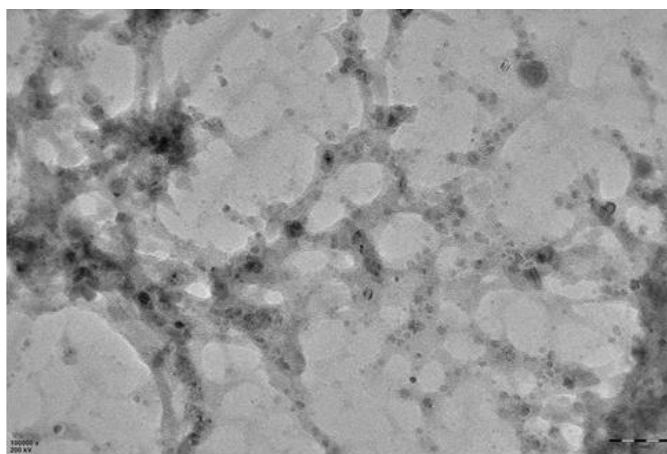


**Figure 3.** TEM characterization of PDTPA-EG@CdTe

### 3.4 The CV characterization of the immobilization and hybridization process of DNA

Cyclic voltammetry was utilized to show the current changes of the modified electrode during the immobilization and hybridization process of DNA. As shown in Fig. 4, after the modification of the Fe<sub>3</sub>O<sub>4</sub>@Au magnetic nanoparticles, the peak current of the redox reaction of the [Fe(CN)<sub>6</sub>]<sup>3-/4-</sup> (curve b) increases dramatically compared with the bare MGCE, whereas the peak potential decreased. This was because that the Fe<sub>3</sub>O<sub>4</sub>@Au magnetic nanoparticles could increase the specific surface area, as well as the good electrical conductivity of the Au nanocomposites as that of our previous result[27]. After the self-assembly of the DNA1/MCH, the peak current (curve c) decreased apparently. This was because that the negative charged phosphate–backbone structure of the DNA could impede the electron transfer. After the hybridization with DNA2, the peak current of the redox reaction decreased again (curve d), while it dropped again (curve e) after the hybridization with DNA3. With the increase of the negative charge after the hybridization, the electron transfer would be further hindered. After the modification of the PDTPA-EG@CdTe nano-composites, the peak would almost disappear (curve f).

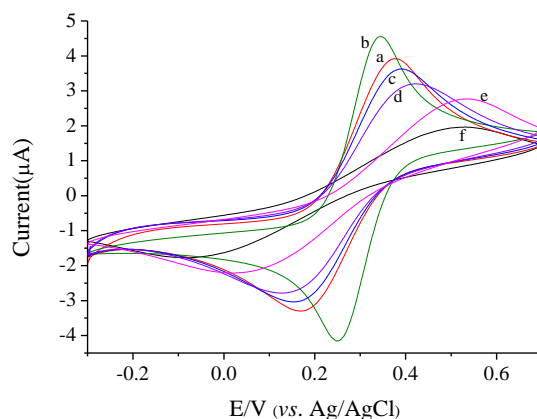


**Figure 4.** Cyclic voltammograms of immobilization and hybridization of SH-ssDNA on electrode (a) bare MGCE; (b) Fe<sub>3</sub>O<sub>4</sub>@Au/bare MGCE; (c) DNA1/MCH; (d) DNA2; (e) DNA3; (f) PDTPA-EG@CdTe; (e) 10 mmol/L [Fe(CN)<sub>6</sub>]<sup>3-/4-</sup>. 0.1 mol/L KCl, scan rate 100 mV/s

### 3.5 The EIS characterization of the immobilization and hybridization process of the DNA

Electrochemical impedance spectroscopy (EIS) is often used to measure the electrochemical response of electrodes with coating. Use the fitting software ZView2 to draw. The semicircle diameter of the Nyquist plot represents the electron transfer resistance (Ret)[28]. As shown in Fig. 5 and Table 1, after the modification of the Fe<sub>3</sub>O<sub>4</sub>@Au magnetic nanoparticles, the resistance of the electron transfer (curve b) decreases dramatically compared with the bare MGCE (curve a). It was due to the specific surface area of the Fe<sub>3</sub>O<sub>4</sub>@Au magnetic nanoparticles and the conductivity of the Au nanoparticles. After the self-assembly of the DNA1/MCH, the Ret increased a lot (curve c) since the phosphate–backbone structure of the DNA would block the [Fe(CN)<sub>6</sub>]<sup>3-/4-</sup> ions.

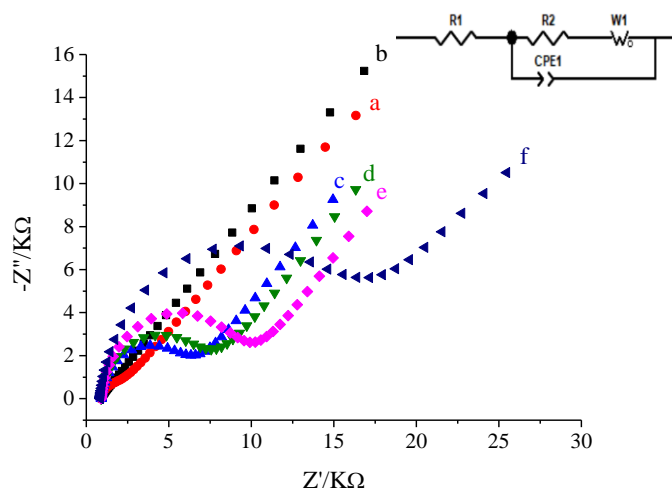


**Figure 5.** Nyquist plots obtained at different modified electrode (a) bare MGCE; (b)  $\text{Fe}_3\text{O}_4@Au$ /bare MGCE; (c) DNA1/MCH/(b); (d) DNA2/(c); (e) DNA3/(d); (f) PDTPA-EG@CdTe/(e) 10 mmol/L  $[\text{Fe}(\text{CN})_6]^{3-/4-}$ . 0.1 mol/L KCl, scan rate: 100 mV/s

Because the dsDNA would enhance this effect, after the hybridization with DNA2, the Ret (curve d) increased again. This may demonstrate that the immobilization and hybridization for the DNAs are occurred naturally. The same phenomenon showed in the hybridization of DNA3 (curve e) after the formation of the sandwich structure. After the immobilization of the PDTPA-EG@CdTe nanocomposites, the negative charge on the electrode surface increased. Since the bare carboxyl group of the PDTPA-EG@CdTe nanocomposites had repel effect towards the  $[\text{Fe}(\text{CN})_6]^{3-/4-}$  ions, the Ret (curve e) also increased apparently. The resistance values for the electrode modified process were shown in table 1.

**Table 1.** Impedance values of different modified electrodes

Curve	a	b	c	d	e	f
Ret( $\Omega$ )	1087	894.4	4971	6021	8347	14316

### 3.6 The repeatability of the ECL behavior of the PDTPA-EG@CdTe nanocomposites

ECL assay was performed for the determination of the PDTPA-EG@CdTe nanocomposites labeled DNA. CV was performed for 10 times. The results showed that the ECL signal had good repeatability (RSD=0.98%). This illustrates that the ECL signal of PDTPA-EG@CdTe nanocomposites labeled DNA was very stable and it could be performed for the DNA detection.

### 3.7 Optimization of the experimental parameter

The dosage of the magnetic nanoparticles and the DNA assembly time were evaluated. As shown in Fig. 6a, when the dosage of magnetic nanoparticles was 2.5  $\mu\text{L}$ –10  $\mu\text{L}$ , the intensity of the

ECL signal gradually increased with the increase of the dosage until reaching a platform, and did not change after 10  $\mu\text{L}$ . So, 10  $\mu\text{L}$  was chosen as the dosage of the magnetic nanoparticles.

DNA1 was immobilized on the surface of  $\text{Fe}_3\text{O}_4@\text{Au}$  by the formation of Au-S bond between -SH at the end of DNA1 and the Au. This process was the self-assembly of DNA1. The effect of self-assembly time on the ECL intensity was investigated.

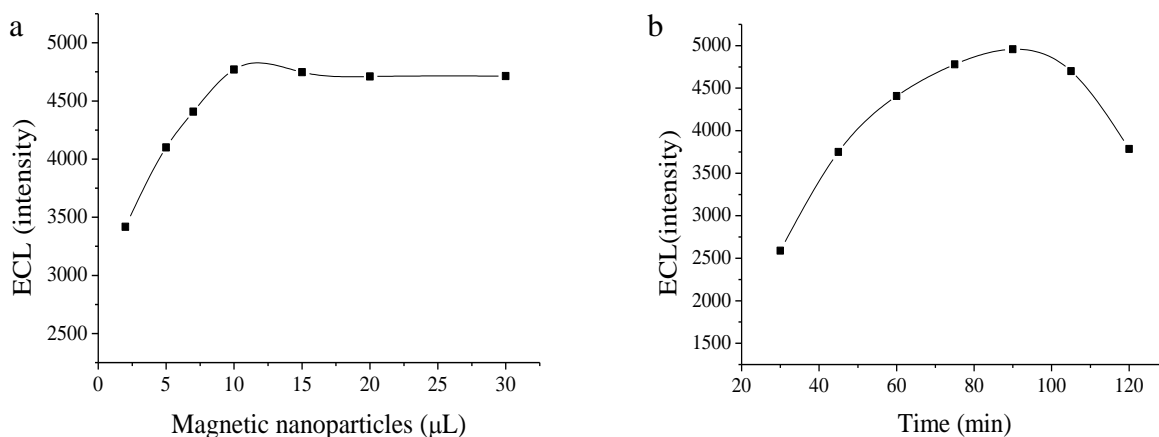


**Figure 6.** The dosage of magnetic nanoparticles (a) and self-assembly time (b)

The relationship between hybridization signal (ECL strength after hybridization) and self-assembly was obtained and the result was shown in Fig.6b. In the range of 0.5 ~ 1.5h, the ECL intensity increased gradually with the increase of self-assembly time, and reached the maximum at 1.5h. Then the efficiency of the hybridization and the response signal decreased after 1.5 h, which might be owing to the reason that the accumulation of the DNA layer could increase the hindrance of the space and static electricity. The results were agreed with those in the reference[29]. So the assembly time was chosen as 1.5 h in the assay.

### 3.8 Calibration curve and detection limit

Under optimized conditions, the ECL signals corresponding to changes of target DNA concentrations were shown in Fig. 7. The intensity of the ECL signal ( $I$ ) was proportional to the DNA concentration ( $c$ ) in the range from  $1.0 \times 10^{-16}$  mol/L to  $1.0 \times 10^{-14}$  mol/L with an equation of  $I = 167.16c + 262.63$  and a correlation coefficient of  $r = 0.9965$ . The detection limit was  $3.0 \times 10^{-17}$  mol/L at a signal-to-noise ratio of 3. In addition, Table 2 lists some parameters of methods for DNA detection based on the signal amplification based on nanoparticle reported. In the reference [31-35], gold nanoparticles (AuNPs) are composited with other nanomaterials as signal probes to detect DNA, which improves the sensitivity of the sensor to a certain extent. At the same time, graphene, as a material with large specific surface area and good electrical conductivity, is also often used to combine with other nanomaterials such as AuNPs, CdSe quantum dots and Cu-MOF for signal amplification of DNA biosensors [19, 30, 34, 36]. For example, the sensitive of DNA detection using

polydiallyldimethylammonium chloride (PDDA) as a carrier loaded with graphene oxide (GO) and AuNPs as signal probes can reach a detection limit of  $3.5 \times 10^{-12}$  mol/L [19]. However, compared with the results of this experiment, it can be clearly seen that the detection limit of the proposed  $\text{Fe}_3\text{O}_4@Au/MGCE$  sensor was much lower than that reported in the references [19, 30-36]. The higher sensitivity was obviously due to the signal amplification strategy based on dendrimers combined with quantum dots.

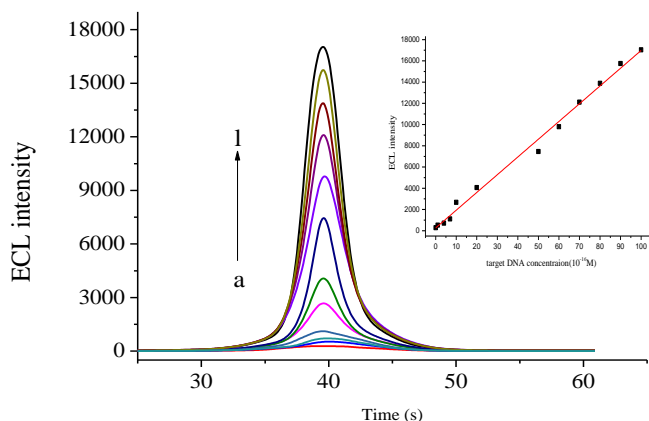


**Figure 7.** Electrochemiluminescence signal recorded under different concentrations of target DNA (the inset figure was calibration curve). From a to l: 0, 1.0, 4.0, 7.0, 10.0, 20.0, 50.0, 60.0, 70.0, 80.0, 90.0, 100.0  $\times 10^{-16}$  mol/L, respectively.

**Table 2.** Comparison of the analytical performances of the methods for DNA detection based on nanoparticle compound

DNA immobilization	Method	Linear range(pmol/L)	DL(mol/L)	References
Cu-MOF/GO/GCE	DPV	$5.0 \times 10^{-14}$ - $1.0 \times 10^{-8}$	$5.2 \times 10^{-15}$	[30]
PDA/Au	LSV	$1.0 \times 10^{-13}$ - $1.0 \times 10^{-8}$	$5.2 \times 10^{-15}$	[31]
Au@Bi <sub>2</sub> S <sub>3</sub> /GCE	EIS	$1.0 \times 10^{-14}$ - $1.0 \times 10^{-9}$	$2 \times 10^{-15}$	[32]
TiO <sub>2</sub> /Au/FTO	PEC	$1.0 \times 10^{-14}$ - $1.0 \times 10^{-7}$	$3 \times 10^{-15}$	[33]
GO/AuNPs/GCE	DPV	$6.0 \times 10^{-11}$ - $6.0 \times 10^{-10}$	$2.7 \times 10^{-11}$	[34]
AuNPs/ZnO/GCE	DPV	$2.5 \times 10^{-12}$ - $2.5 \times 10^{-10}$	$1.8 \times 10^{-12}$	[35]
PDDA-GO QDs/Au	ECL	$1.0 \times 10^{-12}$ - $1.0 \times 10^{-6}$	$1.0 \times 10^{-13}$	[36]
PDDA/GO/Au	ECL	$1.0 \times 10^{-11}$ - $1.0 \times 10^{-6}$	$3.5 \times 10^{-12}$	[19]
$\text{Fe}_3\text{O}_4@Au/MGCE$	ECL	$1.0 \times 10^{-16}$ - $1.0 \times 10^{-14}$	$3.0 \times 10^{-17}$	This work

DPV-differential pulse voltammetry; LSV-linear sweep voltammetry; EIS-electrochemical impedance spectroscopy; PEC-photoelectrochemical

### 3.9 Selectivity of the method

The complementary DNA sequence, single-base, three-base mismatch sequences DNA sequence and noncomplementary DNA sequences were used to evaluate the sensitivity of the method. ECL signal was recorded after hybridization with the three DNA sequences separately and shown in Fig. 8. The ECL intensity produced by the single-base and three-base mismatch DNA were only 8.52% and 6.11% of that of the complementary DNA sequence, and the ECL intensity of the noncomplementary DNA sequence was only 4.12% of that of complementary DNA sequence. Obviously, mismatched DNA was difficult to hybridize with DNA1. Therefore, only the complementary target DNA can produce a sensitive ECL response, that was to say, the method had excellent discrimination ability to single-base mismatched DNA, three-base mismatched DNA and noncomplementary DNA. The results showed the good selectivity of the method.

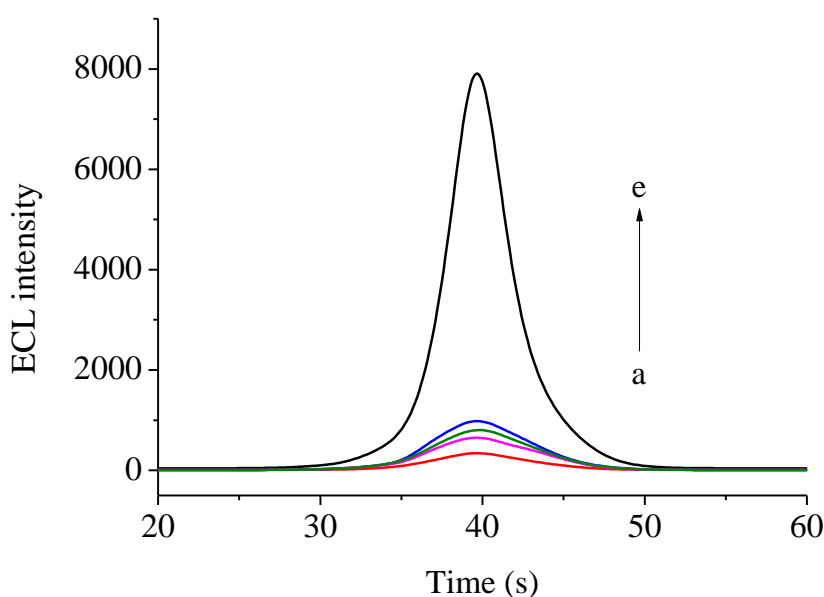


**Figure 8.** Effect of (a) blank sample (without target DNA); (b) noncomplementary sequence; (c) three-base mismatch sequence; (d) one-base mismatch sequence; (e) complementary sequence on ECL intensity

### 3.10 The reproducibility of the method and the stability of PDTPA-EG@CdTe

The reproducibility of the method was evaluated by determination of DNA added in a serum samples.  $\text{Fe}_3\text{O}_4@Au$  magnetic particles was attached on the MGCE surface, and the target DNA with a concentrations of  $5.0 \times 10^{-15}$  mol/L in serums were determined according to the experimental method. Five measurements were performed under the same conditions. After each determination, the magnetic composite particles were removed by taking the magnet away from the surface of MGCE, and then the electrode was put in a 0.5 mol/L HCl stirring for 20-30 s to renew the electrode surface. The relative standard deviation of the measured signals was 4.56% ( $n=5$ ), indicating that the reproducibility of the

method was satisfactory. The stability of PDTPA-EG@CdTe was checked. The synthesized PDTPA-EG@CdTe composite was stored in a refrigerator at 4°C, and taken out at regular intervals as a signal probe to detect the target DNA. The results showed that the ECL signal did not significantly change when the PDTPA-EG@CdTe composite was stored for three months, indicating that the prepared PDTPA-EG@CdTe was highly stable.

### 3.11 Real Sample Analysis in Human Serum

To evaluate the practical application of the method, the human serum samples were centrifuged at 3000 rpm for 10 minutes. Then the supernatants were taken and target DNA in different concentrations were added. The contents of target DNA were assayed and the results are shown in Table 3. It can be seen that the recoveries obtained were in the range of 93.2-101.0%, indicating that the method can be used for DNA determination in actual samples.

**Table 3.** Determination of target DNA in human serum samples

Sample	Added(mol/L)	Found	RSD (% , n=5)	Recovery (%)
1	$2.00 \times 10^{-15}$	$1.92 \times 10^{-15}$	3.27	96.0
2	$5.00 \times 10^{-15}$	$4.66 \times 10^{-15}$	4.56	93.2
3	$1.00 \times 10^{-14}$	$1.01 \times 10^{-14}$	1.17	101.0

## 4. CONCLUSIONS

A unique PDTPA-EG@CdTe nanoclusters with a uniform spatial grid entrapped with large amount of CdTe QDs were synthesized as the ECL probe to labeled on the capture DNA to amplify the ECL signal of DNA determination. In addition, the core-shell Fe<sub>3</sub>O<sub>4</sub>@Au was used to prepare DNA modified electrode with high-efficiency separation and enrichment properties. It provides one strategy for high sensitive and selective assay of specific gene sequences in early cancer diagnosis.

## ACKNOWLEDGEMENTS

The authors gratefully acknowledge the financial support from the Natural Science Foundation of Guangxi Province of China (No. 2021GXNSFAA196011), and the project of Guangxi Key Laboratory of Electrochemical and Magnetochemical Function Materials (No. EMFM20211110).

## References

1. G. Dharanivasan, D. M. I. Jesse, T. Rajamuthuramalingam, G. Rajendran, S. Shanthi and K. Kathiravan, *ACS Omega*, 4 (2019) 10094.
2. S. P. Liang, G. C. He, J. N. Tian, Y. C. Zhao and S. L. Zhao, *Microchim. Acta*, 185 (2018) 119.
3. A. Benvidi, N. M. Saucedo, P. Ramnani, C. Villarreal, A. Mulchandani, M. D. Tezerjani, and S.

- Jahanbani, *Electroanalysis*, 30 (2018) 1791.
4. X. K. Zheng, L. Y. Zhao, D. X. Wen, X. L. Wang, H. X. Yang, W. S. Feng and J. M. Kong, *Talanta*, 207 (2020) 120290.
  5. B. Guo, B. Wen, W. Cheng, X. Y. Zhou, X. L. Duan, M. Zhao, Q. F. Xia and S. J. Ding, *Biosens. Bioelectron.*, 112 (2018) 120.
  6. H. T. Yang, Y. Li, D. Z. Wang, Y. Liu, W. Wei, Y. J. Zhang, S. Q. Liu and P. Li, *Chem. Commun.*, 55 (2019) 5994.
  7. D. L. Chen, M. Zhang, F. Y. Zhou, H. Hai and J. P. Li, *Microchim. Acta*, 186 (2019) 628.
  8. J. T. Cao, J. J. Yang, L. Z. Zhao, Y. L. Wang, H. Wang, Y. M. Liu and S. H. Ma, *Biosens. Bioelectron.*, 99 (2018) 92.
  9. J. Ma, L. Wu, Z. H. Li, Z. C. Lu, W. M. Yin, A. X. Nie, F. Ding, B. R. Wang and H. Y. Han, *Anal. Chem.*, 90 (2018) 7415.
  10. M. Zhang, H. Hai, F. Y. Zhou, J. C. Zhong and J. P. Li, *Chin. J. Anal. Chem.*, 46 (2018) 203.
  11. H. Zhou, T. Q. Han, Q. Wei and S. S. Zhang, *Anal. Chem.*, 88 (2016) 2976.
  12. Y. Zhao, Z. Li, Q. Kuang and G. F. Jie, *J. Electroanal. Chem.*, 812 (2018) 68.
  13. I. A. Olayiwola, B. Mamba and U. Feleni, *Mater. Chem. Phys.*, 244 (2020) 122641.
  14. C. Lu, X. F. Wang, J. J. Xu and H. Y. Chen, *Electrochem Commun.*, 10 (2008) 1530.
  15. B. Babamiri, R. Hallaj and A. Salimi, *Sens. Actuat. B. Chem.*, 254 (2018) 551.
  16. S. Ghosh, D. Ghosh, P. K. Bag, S. C. Bhattacharya and A. Saha, *Nanoscale*, 3 (2011) 1139.
  17. G. F. Jie, J. X. Yuan and J. Zhang, *Biosens Bioelectron.*, 31 (2012) 69.
  18. L. Li, C. C. Niu, T. Li, Y. F. Wan, Y. Zhou, H. J. Wang, R. Yuan and P. Liao, *Biosens Bioelectron.*, 101 (2018) 206.
  19. L. Tan, J. J. Ge, M. Jiao, G. F. Jie and S. Y. Niu, *Talanta*, 183(2018) 108.
  20. B. Babamiri, R. Hallaj and A. Salimia, *Biosens. Bioelectron.*, 99 (2018) 353.
  21. A. M. Carnerup, M. L. Ainalem, V. Alfredsson and T. Nylander, *Langmuir*, 25(2009) 12466.
  22. J. P. Li, Q. Xu, C. Fu and Y. Zhang, *Sens. Actuat. B. Chem.*, 185 (2013) 146.
  23. L. P. Wang, Y. B. Huang and Y. H. Lai, *Appl. Surf. Sci.*, 435 (2018) 290.
  24. T. N. Parac-Vogt, K. Kimpe, S. Laurent, C. Piérart, L. V. Elst, R. N. Muller and K. Binnemans, *Eur. Biophys. J.*, 35 (2006) 136.
  25. H. L. Liu, Y. Y. Cui, P. Li, Y. M. Zhou, X. S. Zhu, Y. W. Tang, Y. Chen and T. H. Lua, *Analyst*, 138(2013) 2647.
  26. F. Divsar, *Anal. Bioanal. Chem.*, 411(2019) 6867.
  27. H. Hai, C. P. Chen, D. L. Chen, P. J. Li, Y. Shan and J. P. Li, *Microchim. Acta*, 188 (2021) 125.
  28. N. Ma, J. L. Liu, B. Liu, L. Z. Li, J. M. Kong and X. J. Zhang, *Talanta*, 236(2022) 122840.
  29. T. M. Herne and M. J. Tarlov, *J. Am. Chem. Soc.*, 119 (1997) 8916.
  30. X. F. Lin, X. Lian, B. B. Luo and X. C. Huang, *Inorg. Chem. Commun.*, 119 (2020) 108095.
  31. S. Han, W. Y. Liu, M. Zheng and R. S. Wang, *Anal. Chem.*, 92 (2020) 4780.
  32. F. Gao, J. Song, B. Zhang, H. Tanaka, F. Gao, W. W. Qiu and Q. X. Wang, *Chin. Chem. Lett.*, 31 (2019) 181.
  33. X. P. Liu, J. S. Chen, C. J. Mao, H. L. Niu, J. M. Song and B. K. Jin, *Biosens. Bioelectron.*, 116 (2018) 23.
  34. S. Hajihosseini, N. Nasirizadeh, M. S. Hejazi and P. Yaghmaei, *Mater. Sci. Eng. C.*, 61 (2016) 506.
  35. Z. Hatami, E. Ragheb, F. Jalali, A. M. Tabrizi and M. Shamsipur, *Bioelectrochemistry*, 133 (2020) 107458.
  36. G. T. Jie, Q. Zhou and G. F. Jie, *Talanta*, 194 (2019) 658.